

A MULTISCALE EXAMINATION OF THE 31 MAY 1998 MECHANICVILLE, NEW YORK, TORNADO

Kenneth D. LaPenta¹
NOAA/National Weather Service, Albany, New York
and

Lance F. Bosart, Thomas J. Galarneau Jr., and Michael J. Dickinson
The University at Albany/SUNY

1. Introduction

Tornadoes rated F3 or higher on the Fujita Scale (1981) are rare in eastern New York (NY) and western New England. Since 1950 there have been only six occurrences of F3 or stronger tornadoes. On 31 May 1998, an F3 tornado formed just west of Mechanicville, Saratoga County, NY, and traveled over 50 km before reaching southwest Vermont (VT) as an F2 tornado (Fig. 1). Since significant tornadoes have the potential to produce severe damage and great loss of life, it is incumbent on the National Weather Service (NWS) to provide as much warning as possible for these storms. Although 68 people were injured in the Mechanicville tornado, accurate and timely severe weather outlooks, tornado watches and tornado warnings, and rapid communication of hazardous weather information likely contributed to no lives being lost. Across the entire Northeast on 31 May, there were 5 fatalities and 127 injuries, associated with 32 tornadoes, 264 reports of wind damage and 84 reports of three quarter inch diameter or larger hail (Fig. 2a). Although the Mechanicville tornado developed within a synoptic scale environment already favorable for tornadoes and severe thunderstorms, we will present some limited evidence that terrain-channeled low-level flow in north-south Hudson River Valley and the interaction of the isolated supercell responsible for the Mechanicville tornado with an overtaking squall line may have enhanced the likelihood of tornadogenesis.

2. Synoptic Overview

Severe weather was widespread from the northern Plains across the Great Lakes to New England during late May and early June 1998. During this time, the pattern over North America was dominated by above normal 200 hPa heights from north of Hawaii northward across the Gulf of Alaska, eastward toward Greenland, and over much of the southern half of the United States. Below normal heights were found west of California and over Canada to the south of Hudson Bay. Given the anomalously strong trough (ridge) south of Hudson Bay (over the southern United States), the pattern was conducive to an anomalously strong westerly jet from the northern Rockies to New England. The severe weather threat was maximized where the ascent zones associated with disturbances embedded in the jet intercepted low-level baroclinic regions and warm, moist unstable air.

A 500 hPa closed low moved slowly southward off the west coast of North America from 21 May to 28 May, and then turned northeastward across the northern Rockies. Meanwhile, a second 500 hPa closed low was situated near Hudson Bay from 26 May to 2 June. Short wave energy from these two systems combined to produce a surface cyclone over the northern Plains States on 30 May. The low accelerated east, and then northeast, and by 0000 UTC 1 June was southeast of James Bay and had deepened 13 hPa (to 985 hPa) during the previous 24 h. The severe weather over the northeastern United States on 31 May occurred in the warm sector of this deepening cyclone. Surface and upper-air analyses for 1800 UTC 31 May 1998 were crafted from the Global Reanalysis Data produced by

¹ *Corresponding author address:* Kenneth LaPenta,
National Weather Service, 251 Fuller Rd., Suite B300,
Albany, NY 12203-3640

the NOAA's National Centers for Environmental Prediction (NCEP) and the National Center for Atmospheric Research (NCAR) (Kalnay et al. 1996; Kistler et al. 2001) to provide a synoptic overview of this event (Fig. 3). During the late afternoon and evening of 30 May the storm helped to trigger severe weather over South Dakota where the town of Spencer was devastated by an F4 tornado (Storm Data 1998). A derecho evolved from this convection and moved eastward at more than 30 m s^{-1} across Minnesota, Iowa and Wisconsin, reaching lower Michigan by 0800 UTC 31 May. This derecho produced widespread wind damage (Fig. 2) in association with wind gusts of $30\text{-}40 \text{ m s}^{-1}$ (Storm Data 1998).

The observed 850 hPa winds at Detroit, Michigan (DTX) and Wilmington, Ohio (ILN) at 1200 UTC 31 May were 33 m s^{-1} and 23 m s^{-1} , respectively. This strong low-level flow produced significant warm air advection ($>10^\circ\text{C}$ [18°F] 12 h^{-1}) into the Northeast, helped to advect moisture rapidly into eastern NY during the morning increasing the Convective Available Potential Energy (CAPE), and contributed to strong shear and storm-relative helicity (SRH) in the lower troposphere (section 3). At 250 hPa a coupled jet pattern was evident across the Northeast. Divergence was concentrated in the left exit region of the trailing jet and the right entrance region of the leading jet. By 0000 UTC 1 June, the 250 hPa divergence core associated with the coupled jet was concentrated in an arc from eastern Pennsylvania (PA) to southern Quebec between the coupled jets and above the region of maximum 700 hPa ascent.

Additional short-wave disturbances that rotated around the Hudson Bay closed low also interacted with the anomalously strong upper-level jet and helped to spawn two additional major severe weather outbreaks (29 May and 2 June) over the northeastern United States in addition to the 31 May storms.

3. Mesoscale Environment

a. Morning destabilization

The 1200 UTC 31 May sounding from Detroit (DTX), Michigan, shown in Fig. 4a, was representative of the immediate post-derecho mesoscale environment. A strong corridor of westerly winds (peak speeds $> 35 \text{ m s}^{-1}$) was found in conjunction with the deep mixed layer from 825-700 hPa. The DTX sounding also indicated that the air mass below the mixed layer had stabilized, likely in response to rain-cooled air. Any modification of the

lowest levels of the DTX sounding to make it representative of the warmer and more moist conditions to the east, where strong low-level warm-air advection was occurring, would produce a very unstable air mass. Unfortunately, no representative sounding was available to confirm this hypothesis because there was no Buffalo, NY radiosonde launch for 1200 UTC 31 May due to equipment failure. Instead, we show in Fig. 4b the 1200 and 1800 UTC 31 May soundings from Albany (ALY), NY. A stable pre-warm front environment at 1200 UTC warmed and moistened considerably by 1800 UTC. During the morning, most of the Hudson Valley and New England were under a south and southeasterly flow of relatively cool marine air with surface dew points generally under 15°C (59°F). A southwesterly flow across PA and western/central NY marked the leading edge of the advancing warmer, moister and unstable air mass. Surface θ_e values exceeded 340 K by 1500 UTC across western NY and PA with an area in excess of 348 K in the clear air (Fig. 5b) over southeastern PA as solar heating combined with the transport of increasingly warmer and moister air to destabilize the air mass (surface-based LIs had decreased to -5 to -8 in this region).

At 1700 UTC, satellite visible imagery showed thick cloudiness with a large area of showers and embedded thunderstorms from northern NY to northeastern Ohio (Fig. 5c). This area of clouds and precipitation was associated with the remnants of the derecho that crossed portions of the Great Lakes the previous night. As this convection moved eastward across NY, thunderstorms reignited between 1700-2000 UTC (Fig. 5d)

b. Environment for supercell growth over complex terrain

As the afternoon of 31 May 1998 progressed, the atmosphere across eastern NY became increasingly favorable for severe weather. By 2000 UTC the warmer and moister unstable air had overspread the Hudson Valley and much of interior southern New England with θ_e values $> 348 \text{ K}$ being common (Fig. 6). Surface temperatures in the clear air ahead of the developing thunderstorms were in the $27\text{-}32^\circ\text{C}$ ($81\text{-}90^\circ\text{F}$) range with dew points between $18\text{-}20^\circ\text{C}$ ($64\text{-}68^\circ\text{F}$). The 1800 UTC radiosonde observation at ALY (Fig. 4b), located about 6 km south of ALB, was modified for the observed ALB surface temperature and dew point temperature at 2000 UTC. The SBCAPE (mean layer CAPE [MLCAPE]) increased to about 2000 J kg^{-1} (1600 J kg^{-1}). The lifting condensation level (MLLCL, based on lifting a parcel with conditions averaged over the

lowest 100 hPa) was about 1200 m. Thompson et al. (2003) showed an average MLLCL for significant tornado, weak tornado and non-tornadic supercell cases, of about 1000 m, 1200 m and 1350 m respectively.

The shear magnitude was 31 m s^{-1} in the 0-6 km above ground layer (AGL). Observations and modeling studies (e.g., Weisman and Rotunno 2000) indicate that vertical wind shear greater than $20\text{-}25 \text{ m s}^{-1}$ is favorable for the development of long-lived convective structures such as supercells. Based on observed storm motion of 260° at 21 m s^{-1} , the SRH was greater than $450 \text{ m}^2 \text{ s}^{-2}$. Davies-Jones et al. (1990) indicated this SRH value would be large enough to support significant (F2 and greater) tornadoes. Recent studies using Rapid Update Cycle model generated proximity soundings (Thompson et al. 2003) and observed proximity soundings (Rasmussen 2002) suggest that shear and SRH in the 0-1 km AGL layer are better at discriminating supercells that produce significant tornadoes from non-tornadic supercells than deep layer (0-6 km shear and 0-3 km SRH) measures of these parameters. The SRH (shear) in the surface to 1 km AGL layer was about $140 \text{ m}^2 \text{ s}^{-2}$ (14 m s^{-2}). The 0-1 km SRH was slightly below the average ($165 \text{ m}^2 \text{ s}^{-2}$) for significant tornadoes in Thompson et al. (2003) but it was above the average ($89 \text{ m}^2 \text{ s}^{-2}$) for tornadic storms in Rasmussen (2002). Based on Rasmussen (2002), the combination of MLCAPE and 0-1 km SRH pointed to the possibility of tornadoes.

While conditions in the warm sector of this storm were favorable for the development of severe storms and tornadoes, terrain may have played a role in further enhancing the tornadic potential in the immediate Hudson Valley. A number of significant physiographic features are present in eastern NY and western New England. To the west of the north-south oriented Hudson Valley are the Catskill and Adirondack mountains (Fig. 1). These two mountain ranges are separated by the east-west oriented Mohawk Valley. To the east of the Hudson Valley in western New England are the Green (VT) and Berkshire (Massachusetts) Mountains. On this day, terrain channeling of the southerly low-level flow within the Hudson Valley may have helped advect warm, moist air northward. Figure 7a shows time series of temperature, dewpoint, pressure and wind from KALB. It shows a steady increase in dewpoint through the day, and the maintenance of a due south wind flow until convection arrived shortly after 2000 UTC. This southerly flow transported high θ_e northward. The 1900 UTC θ_e analysis shows an axis of higher θ_e air extending northward within the

Hudson Valley (Fig. 8). This pattern of higher θ_e air in the Hudson Valley with a south or southwest low-level wind flow is common, and is also seen in higher resolution operational numerical models.

The near surface flow west of the Hudson Valley was generally out of the south-southwest. This south-southwest flow was channeled into a more southerly direction at low-levels within the immediate Hudson Valley. Fig. 7b compares the surface wind direction at KALB and Schenectady (KSCH) located in the Hudson Valley with the surface wind direction at Utica (KUCA) and Binghamton (KBGM) located west of the Hudson Valley. KBGM consistently had a more westerly component to the surface wind than Hudson Valley locations. At KUCA the surface wind was from the southeast (up the Mohawk Valley, see Fig. 1) prior to 1500 UTC. Once in the warm sector, however, the wind at UCA showed a greater westerly component than at Hudson Valley locations. The channeling of the surface wind in the Hudson Valley to a more southerly direction resulted in an increase in the shear and SRH. The channeling of a southwest flow to a southerly flow within the Hudson Valley is a common occurrence as indicated by the wind rose for KALB in Fig7c taken from Wasula et al. (2002).

A 6 h NCEP ETA forecast (the model was initialized at 1500 UTC with 32 km resolution) of 975 hPa winds valid at 2100 UTC showed evidence of terrain channeling. The winds in the Hudson Valley, especially near and just south of Mechanicville, were more southerly than in surrounding areas to the west and to the east. This helped maximize the 0-6 km shear (29 m s^{-1}) just south of Mechanicville (not shown). While large scale conditions supported the possibility of tornadoes (e.g., Rasmussen 2003; Johns and Doswell 1992; Davies-Jones et al. 1990), a storm moving from the northern Catskills into the Hudson Valley would encounter a somewhat more unstable air mass with greater shear in the lower troposphere due to terrain channeling.

4. Evolution of the Mechanicville Tornado

a. Radar Analysis

The remnants of the derecho that crossed Michigan during the early morning hours of 31 May reached western NY at 1600 UTC. The convection then intensified as it moved east, producing locally severe weather as it reached central NY by 1824 UTC, about two hours prior to the Mechanicville tornado (2022 UTC). At 1824 UTC, a small cluster

of isolated storms developed about 55 km to the east of the line. One of the storms in this cluster intensified by 1906 UTC as it moved east-northeast. By 1946 UTC the intensifying line began to bow down the Mohawk Valley as it was catching up with the still intensifying leading supercell storm (Fig. 9a). This leading storm, only about 30 km ahead of the line, had become severe (downed trees were reported) as it approached the Hudson Valley north of ALY.

North of the apex of the squall line that was bowed down the Mohawk Valley, there was evidence of a line echo wave pattern (LEWP), a region of cyclonic vorticity and an embedded mesoscale vortex as seen in the KENX base reflectivity and storm-relative velocity (SRM) imagery at 1946 UTC (Fig. 9). Inbound flow along the Fulton/Montgomery County line and outbound flow just to the east suggests the presence of a region of mesoscale cyclonic vorticity at the northern end of the advancing squall line in a location where a northern book-end vortex would likely be found if present (estimated rotational velocity at this time was about 14 m s^{-1}). Just to the east, the leading supercell continued to intensify as it approached the confluence of the Mohawk and Hudson Valleys. This intensification may have been related to the presence of a slightly more unstable and more highly sheared environment in the Hudson Valley and/or the ongoing interaction of the overtaking squall line with the leading. Tornadogenesis occurred at 2022 UTC, about the time the outflow from the line of storms to the west merged with the leading severe storm. This outflow was likely channeled east-southeastward down the Mohawk Valley. KENX base velocity data at 1957 UTC (25 min before tornadogenesis) indicated an area of higher winds in this storm-initiated outflow moving down the Mohawk Valley.

At 2002 UTC, 20 minutes prior to the tornado, weak convergence was indicated in the SRM data about 1 km above mean sea level (MSL) in the KENX 0.5° beam angle volume scan (not shown). Above 1 km, cyclonic rotation increased with height, reaching 21 m s^{-1} at 3-4 km MSL. By 2012 UTC, strong rotation ($21\text{-}23 \text{ m s}^{-1}$) had descended toward the surface, but at the lowest elevation scan (about 1 km MSL) convergent rotation was present. At that time, the outflow from the line of severe storms approaching from the west had reached the storm. At 2017 UTC, strong rotation reached the lowest elevation scan (0.5°), but inbound and outbound velocity maxima were still separated by about 2 km. The first tornado damage occurred at 2022 UTC, and at that time the radar showed a maximum gate-to-

gate rotational velocity of 28 m s^{-1} at 0.5° (Fig. 10a). The WSR-88D first identified a tornado vortex signature (TVS) based on the volume scan beginning at 2022 UTC, although it should be noted that the TVS information was not available to forecasters until several minutes after the completion of the volume scan, or at about 2030 UTC. The tornado reached its greatest intensity shortly after formation in Saratoga County, NY. It moved east across northern Rensselaer County, NY, before dissipating in Bennington County, VT, (F2 intensity) with a total path length of 48 km (Fig. 1).

b. Lightning analysis

Cloud-to-ground (CG) lightning flash rates and distributions were also examined to document the interaction of the overtaking squall line with the isolated supercell that eventually spawned the Mechanicville tornado. Our analysis was motivated by previous CG lightning studies (e.g., Kane 1991; Seimon 1993; MacGorman and Burgess 1994; Galarneau et al. 2000; Gilmore and Wicker 2002) that suggested that tornadic supercell thunderstorms can have distinct lightning flash rates and polarity signatures. We used CG flash data obtained from the National Lightning Detection Network (NLDN) to construct a time series of CG flashes in the advancing squall line and the isolated supercell beginning approximately two hours prior to tornado formation at 2022 UTC. We also mapped the storm-relative distribution of CG flashes in 10 min periods beginning 2002 UTC in an effort to identify possible spatial variations in CG flash activity during the interaction of the squall line and isolated supercell.

In order to construct Fig. 11a, CG lightning flash data obtained from the National Lightning Detection Network (NLDN) were plotted on a topographic map. These CG flashes were tabulated separately and assigned to either the squall line or the isolated supercell. We estimate that the subjective tabulation procedure had small margin of error ($\pm 1\text{-}2$ flashes per count) prior to squall line and supercell merger, and a larger margin of error ($\pm 5\text{-}10$ flashes per count) subsequently. The separation distance between the squall line and supercell was calculated using the KENX Doppler radar reflectivity images and was measured from the core of highest reflectivities in the squall line to the supercell mesocyclone. The 10 min distributions of CG lightning flashes shown in Fig. 11b were displayed using Sigma Plot 5.0 on a horizontal map relative to the position of the KENX Doppler radar indicated-mesocyclone (tornado) prior to tornadogenesis (subsequent to tornadogenesis). The analysis domain

was 70 km x 80 km (5600 km²) and was centered on the mesocyclone (or tornado). The number of CG lightning flashes, denoted in the lower right corner of each panel, was counted objectively by Sigma Plot 5.0. The CG flash numbers were not normalized because the relative length of the squall line within the analysis domain did not change during the 40 min period shown in Fig. 11b (i.e. the overall area of the horizontal map covered by electrically active convection changed little with time).

Until about 1855 UTC the CG flash rate in the isolated supercell remained under 10 flashes per 5 min during which time the squall line remained 40-45 km to the west of the supercell (Fig. 11a). Subsequent to 1855 UTC the squall line accelerated eastward relative to the isolated supercell, closing to within 10 km by 2005 UTC. Over this 80 min period the supercell flash rate first increased slowly to 10-15 CG flashes per 5 min period and then more rapidly to more than 20 CG flashes per 5 min after 1950 UTC. Beginning at 2010 UTC the CG flash rate increased to 20 flashes per 2 min (note time interval reduction beginning at 2010 UTC) through 2014 UTC during which time the advancing squall line reached to within 6-7 km of the supercell. A brief decrease in the CG flash rate from 2014-2018 UTC was followed by an increase to almost 25 flashes per 2 min by 2022 UTC. Subsequent to tornadogenesis at 2022 UTC, the CG flash rate continued to increase to more than 35 flashes per 2 min. Note also that the percentage of positive flashes generally remained under 10 % (except 12% near 1905 UTC), but was briefly near zero at the time of tornadogenesis.

Maps of the storm-relative CG flash distribution are shown in Fig. 11b. A clear separation can be seen between the CG flashes in the overtaking squall line and the leading isolated supercell between 2002 and 2012 UTC. The few positive CG flashes were concentrated mostly along the northern half of the squall line. By 2022 UTC (tornado formation) the overall number of CG flashes in 10 min had increased from 253 to 461. This increase in CG flash rate occurred as the squall line overtook the supercell (it was still possible to distinguish the CG activity with each feature). Between 2022 and 2032 UTC the overall number of CG flashes increased further to 664 but it was more difficult to distinguish between squall line- and supercell-related CG flashes as merger of the two systems had occurred. Likewise, the number and percentage of positive CG flashes increased through 2042 UTC, particularly in close proximity (within 10-15 km) of the tornado. The CG flashes were concentrated mostly to the left of the storm track, primarily in the forward flank downdraft region of the supercell prior to tornadogenesis (Lemon

and Doswell 1979) and merger with the squall line. Subsequent to tornadogenesis and merger the CG flashes were concentrated in the left-rear and right-rear quadrants relative to the storm track. Overall, the results from Fig. 11 suggest that as the squall line bowed down the Mohawk Valley and overtook the leading supercell there was a significant increase in the CG flash rate which continued subsequent to tornadogenesis at 2022

5. Discussion

While most supercells produce severe weather, less than half produce tornadoes (e.g., Thompson et al. 2003; Brooks et al. 1994). Several studies (e.g., Thompson et al. 2003; Rasmussen 2002; Brooks et al. 1994) have attempted to identify meteorological conditions that differentiate environments that produce tornadic supercells and non-tornadic supercells. Although atmospheric conditions on 31 May 1998 favored the development of supercells and tornadoes, the critical question is what physical mechanisms may have contributed to the actual tornadogenesis process. We have attempted to address this question through an examination of the available observations. Our results suggest that antecedent terrain-channeled southerly flow in the Hudson Valley may have played a role in tornadogenesis. This terrain-channeled southerly flow was backed relative to the more southwesterly flow over the higher terrain of the Catskills to the west of the Hudson Valley and contributed to lengthened and more clockwise turning hodographs in the Hudson Valley. As the supercell that spawned the Mechanicville tornado reached the juxtaposition of the western edge of the Hudson Valley with the eastern end of the Mohawk Valley, it may have been influenced by the terrain-channeled low-level southerly flow in the Hudson Valley and the higher θ_e air being advected northward that was also increasing the instability in the valley.

A second factor that may have contributed to tornadogenesis was the effect of differential roughness (friction) over complex terrain. The frictional effects of terrain are greatest near the surface and decrease upward. In regions of complex terrain (e.g., mountainous regions with deep river valleys) large mesoscale gradients of vorticity are possible in conjunction with differential roughness. Regions where this mesoscale vorticity is concentrated on days when the large-scale environment is favorable for severe weather may be conducive to tornadogenesis (e.g. where the river valleys produce terrain-channeled backed low-level flow relative to mid-level flow). The highest peaks of the Catskill Mountains rise to a little above 1200 m

MSL, indicating the impact of the terrain channeled flow will be most significant in the critical 0-1 km layer. Increased shear in the lowest km above the ground has been shown to be favorable for tornadogenesis in idealized modeling studies (e.g., Wicker 2000; Wilhelmson and Wicker 2001), and in studies using model-generated (Thompson et al 2003) and observed soundings (Rasmussen 2003) near supercells.

A third factor that may have played a role in tornadogenesis was the interaction of an overtaking squall line with a leading isolated supercell. The storm that produced the Mechanicville tornado developed over 50 km ahead of a line of severe storms to the west (1824 UTC). Just prior to the tornado (2022 UTC), the outflow from the line of storms to the west merged with the supercell. The interaction may have increased low-level horizontal vorticity and contributed to tornadogenesis. Goodman and Knupp (1993), Bullas and Wallace (1988), Hamilton (1969) and Cook (1961) have documented cases where tornadoes formed after this type of interaction. Goodman and Knupp (1993) examined the Huntsville, Alabama, tornado (F4) of 15 November 1989. They postulated that the interaction between the squall line gust front and the supercell mesocyclone intensified low-level vorticity and was responsible for the observed rapid intensification of the tornado. However, they could not resolve whether tornadogenesis was triggered by the squall line gust front or by the supercell's rear flank downdraft. The Edmonton, Alberta, Canada tornado (F4) on 31 July 1987 developed in a similar fashion (Bullas and Wallace 1988). Hamilton (1969) summarized the work of Cook (1961) concerning cases where cells developed ahead of, and eventually merged with a line of thunderstorms. Tornadoes occurred in 8 of 11 cases where the advance cell was intense. In these cases, gust front boundaries appeared to have intensified low-level vorticity thereby strengthening an existing tornado or providing the impetus for tornadogenesis (Goodman and Knupp 1993). Other studies have shown the importance of boundary interaction in tornado formation, although in these studies squall line-supercell interactions were not present in all cases. In a study of 86 tornadoes in the northeastern United States, LaPenta et al. (2000) indicated radar detectable boundaries were present in about a fifth of the cases. Nearly 70% of significant tornadoes in the VORTEX-95 experiment (Markowski et al. 1998) occurred near preexisting mesoscale boundaries.

A different perspective on the possible interaction of a squall line and an isolated supercell

comes from an idealized simulation of a quasi-linear convective system by Weisman and Davis (1998). In an experiment with Coriolis effects included, they showed that well-defined backed flow was prevalent at the 2 km level ahead of a northern book-end vortex 4.5 and 6 h into the simulation (their Fig. 4). This result, repeated in Weisman (2001; his Fig. 22), prompts us to suggest that if such a region of low-level backed flow ahead of a northern book-end vortex were to begin overtaking an isolated supercell downstream that the immediate supercell environment might be especially favorable for tornadogenesis. A future idealized simulation of a squall line with a northern book-end vortex overtaking a leading isolated supercell modeled after the Mechanicville tornado case might prove to be enlightening. In this context, the overtaking squall line and its associated northern book-end vortex can be regarded as an external influence on tornadogenesis on a day when the atmospheric environment favored supercells and tornadoes over the Northeast. A schematic synopsis of how the overtaking northern book-end vortex and squall line might have interacted with the leading isolated supercell and low-level terrain-channeled southerly flow in the Hudson Valley is offered in Fig. 24.

Forecast issues were also raised by the Mechanicville tornado event. Recognizing that synoptic scale conditions were favorable for severe thunderstorms and tornadoes on 31 May 1998 was the first step in alerting the public to the potential for dangerous weather. The Storm Prediction Center had indicated a *high risk* of severe thunderstorms and tornadoes for parts of the Northeast. A local study (Maglaras and LaPenta 1997) supported the tornadic threat, and strongly worded statements were issued alerting the public to the dangerous situation. Previous research on the GBR tornado event (Bosart et al. 2004; manuscript submitted to *Wea. Forecasting*), a storm similar to the Mechanicville tornado, provided meteorologists an understanding of the potential role of terrain and mesoscale processes in supercell intensification. It also provided experience in radar-based detection of tornado formation. Being aware of the mesoscale environment, and the role terrain can play in modifying it, can be important in maximizing warning lead time. This is especially true in locations where tornadoes are infrequent. A Tornado Watch was issued nearly two hours prior to the Mechanicville tornado and a Tornado Warning was issued with 39 minutes lead time. The large lead time can be attributed to a number of factors. The city of Mechanicville lies in the extreme eastern portion of Saratoga County, NY. As the storm moved east and

neared the western portion of the County, about 40 km to the west of Mechanicville, a warning decision had to be made. Radar and spotter reports indicated at least a severe thunderstorm warning was necessary. While the radar did not indicate a tornado at that time, a tornado warning was issued based on a number of factors. A tornado watch was in effect and the SPC had indicated a high risk of severe storms. The storm was already severe and a spotter reported a tornado about 9 km west of the Saratoga County line. The KENX radar is located at an elevation of about 550 m MSL and the radar beam can overshoot shallow features in valleys, so it was difficult to rule out this report. Also, experience and previous research (Bosart et al. 2004, manuscript submitted to *Wea. Forecasting*) indicated the storm was entering an area of somewhat increased instability and shear. The storm continued to intensify as it crossed the county line and as radar indicated the high probability of a tornado, a severe weather statement was issued refining the tornado track and indicating that a “dangerous tornado was moving across Saratoga County...”. F3 tornadoes in upstate NY are relatively rare. Although 68 people were injured in the Mechanicville tornado, accurate and timely outlooks, tornado watches and tornado warnings, and rapid communication of hazardous weather information likely contributed to no lives being lost.

6. Acknowledgements

The authors are grateful to COMET which provided support for research (UCAR COMET Partners Grant #S9773888) that was extremely valuable in supporting the NWS’s timely warnings for the Mechanicville tornado, and was the impetus for the continued research on tornadoes in the Northeast. Research on this storm has continued as parts of the COMET Cooperative Grant UCAR-09915806 and NOAA Grant 1007941-1-012365 awarded to the University at Albany as part of the CSTAR program. Anton Seimon is thanked for making critical comments on the manuscript. The authors would also like to thank Kristen Corbosiero for helping with the figures, Celeste Iovinella for helping to put the manuscript in final form, and the anonymous reviewers from Weather and Forecasting for their many constructive suggestions for improving the manuscript.

7. References

- Brooks, H. E., C. A. Doswell III, and J. Cooper, 1994: On the environment of tornadic and nontornadic mesocyclones. *Wea. Forecasting*, **9**, 606–618.
- Bullas, J. M., and A. F. Wallace, 1988: The Edmonton tornado, July 31, 1987. Preprints, *15th Conference on Severe Local Storms*, Amer. Meteor. Soc., Baltimore, MD., 438–443.
- Cook, B. J., 1961: Some radar LEWP observations and associated severe weather. *Proceedings of the 9th Radar Conference*, Amer. Meteor. Soc., Boston, MA., 181-185.
- Davies-Jones, R. P., D. Burgess, and M. Foster, 1990: Test of helicity as a tornado forecast parameter. Preprints, *16th Conf. on Severe Local Storms*, Kananaskis Park, Alta., Canada, Amer. Meteor. Soc., 588–592.
- Fujita, T. Theodore, 1981: Tornadoes and downbursts in the context of generalized planetary scales. *J. Atmos. Sci.*, **38**, 1511–1534.
- Galarneau, T. J. Jr., S. F. Honikman, A. C. Cacciola, L. F. Bosart, K. D. LaPenta, and J. S. Quinlan, 2000: Lightning in tornadic thunderstorms in the northeastern United States. Preprints, *20th Conf. on Severe Local Storms*, Orlando, FL, Amer. Meteor. Soc., 108–109.
- Gilmore, M. S., and L. J. Wicker, 2002: Influences of the local environment on supercell cloud-to-ground lightning, radar characteristics, and severe weather on 2 June 1995. *Mon. Wea. Rev.*, **130**, 2349–2372.
- Goodman, S. J., and K. R. Knupp, 1993: Tornadogenesis via squall line and supercell interaction: The November 15, 1989, Huntsville, Alabama, tornado. *The Tornado: Its Structure, Dynamics, Prediction, and Hazards*. Geophys. Monogr., **79**, C. Church, D. Burgess, C. Doswell, and R. Davies-Jones, Eds., Amer. Geophys. Union, 183–200.
- Hamilton, R. E., 1969: A review of use of radar in detection of tornadoes and hail, *Tech. Memo. WBTM-ER-34*, Weather Bur. East. Reg. Headquarters, Garden City, N. Y., 64 pp.
- Hart, J., and P. Janish, 1999. SeverePlot v2.0, historical severe weather report database Version 2.0, NWS Storm Prediction Center, Norman, OK. [Available online at <http://www.spc.noaa.gov/software/svrplot2/>]

- Johns, R. H., and C. A. Doswell III, 1992: Severe local storms forecasting. *Wea. Forecasting*, **7**, 588–612.
- Kalnay, E., M. Kanamitsu, R. Kistler, W. Collins, D. Deaven, L. Gandin, M. Iredell, S. Saha, G. White, J. Woollen, Y. Zhu, M. Chelliah, W. Ebisuzaki, W. Higgins, J. Janowiak, K. C. Mo, C. Ropelewski, J. Wang, A. Leetmaa, R. Reynolds, R. Jenne, and D. Joseph, 1996: The NCEP/NCAR 40-Year Reanalysis Project. *Bull. Amer. Meteor. Soc.*, **77**, 437–431.
- Kane, R. J., 1991: Correlating lightning to severe local storms in the northeastern United States. *Wea. Forecasting*, **6**, 3–12.
- Kistler, R., E. Kalnay, W. Collins, S. Saha, G. White, J. Woollen, M. Chelliah, W. Ebisuzaki, M. Kanamitsu, V. Kousky, H. van den Dool, R. Jenne, and M. Fiorino, 2001: The NCEP–NCAR 50-year reanalysis: Monthly means CD-ROM and documentation. *Bull. Amer. Meteor. Soc.*, **82**, 247–268.
- LaPenta, K. D., G. M. Maglaras, J. S. Quinlan, H. J. Johnson, L. F. Bosart, and T. J. Galarneau, Jr., 2000: Radar observations of northeastern United States tornadoes. Preprints, *20th Conf. on Severe Local Storms*, Orlando, FL, Amer. Meteor. Soc., 356–359.
- Lemon, L. R., and C. A. Doswell III, 1979: Severe thunderstorm evolution and mesocyclone structure as related to tornadogenesis. *Mon. Wea. Rev.*, **107**, 1184–1197.
- MacGorman, D. R., and D. W. Burgess, 1994: Positive cloud-to-ground lightning in tornadic storms and hailstorms. *Mon. Wea. Rev.*, **122**, 1671–1697.
- Maglaras, G. J., and K. D. LaPenta, 1997: Development of a forecast equation to predict the severity of thunderstorm events in New York State. *Natl. Wea. Dig.*, **21**, 3, 3–9.
- Markowski, P. M., E. N. Rasmussen, and J. M. Straka, 1998: The occurrence of tornadoes in supercells interacting with boundaries during VORTEX-95. *Wea. Forecasting*, **13**, 852–859.
- Rasmussen, E. N., 2003: Refined supercell and tornado forecast parameters. *Wea. Forecasting*, **18**, 530–535.
- Seimon, A., 1993: Anomalous cloud-to-ground lightning in an F5-Tornado-producing supercell thunderstorm on 28 August 1990. *Bull. Amer. Meteor. Soc.*, **74**, 189–203.
- Thompson, R. L., R. Edwards, J. A. Hart, K. L. Elmore, and P. M. Markowski, 2003: Close proximity soundings within supercell environments obtained from the Rapid Update Cycle. *Wea. Forecasting*, **18**, 1243–1261.
- U.S. Department of Commerce, 1998. *Storm Data*. Vol. 40. National Climatic Data Center. [Available from National Climatic Data Center, Federal Building, 151 Patton Ave., Asheville, NC 28801.] *Amer. Meteor. Soc.*, 255–298.
- Wallace, J. M., and D. S. Gutzler, 1981: Teleconnections in the geopotential height field during the Northern Hemisphere winter. *Mon. Wea. Rev.*, **109**, 784–812.
- Wasula, A. C., L. F. Bosart, and K. D. LaPenta, 2002: The influence of terrain on the severe weather distribution across interior eastern New York and western New England. *Wea. Forecasting*, **17**, 1277–1289.
- Weisman, M. L., 2001: Bow echoes: A tribute to T. T. Fujita. *Bulletin of the Amer. Meteor. Soc.*, **82**, 97–116.
- Weisman, M. L., and R. Rotunno, 2000: The use of vertical wind shear versus helicity in interpreting supercell dynamics. *J. Atmos. Sci.*, **57**, 1452–1472.
- Weisman, M. L., and C. A. Davis, 1998: Mechanisms for the generation of mesoscale vortices within quasi-linear convective systems. *J. Atmos. Sci.*, **55**, 2603–2622.
- Wicker, L. J., 2000: The role of low-level shear, mid-level shear, and buoyancy in the intensity of modelled low-level mesocyclones. Preprints, *20th Conf. on Severe Local Storms*, Orlando FL., Amer. Meteor. Soc., 587–590.
- Wilhelmson, R. B., and L. J. Wicker, 2001: Numerical modeling of severe local storms. *Severe Convective Storms, Meteor. Monogr.*, No. 50, Amer. Meteor. Soc., 123–166.

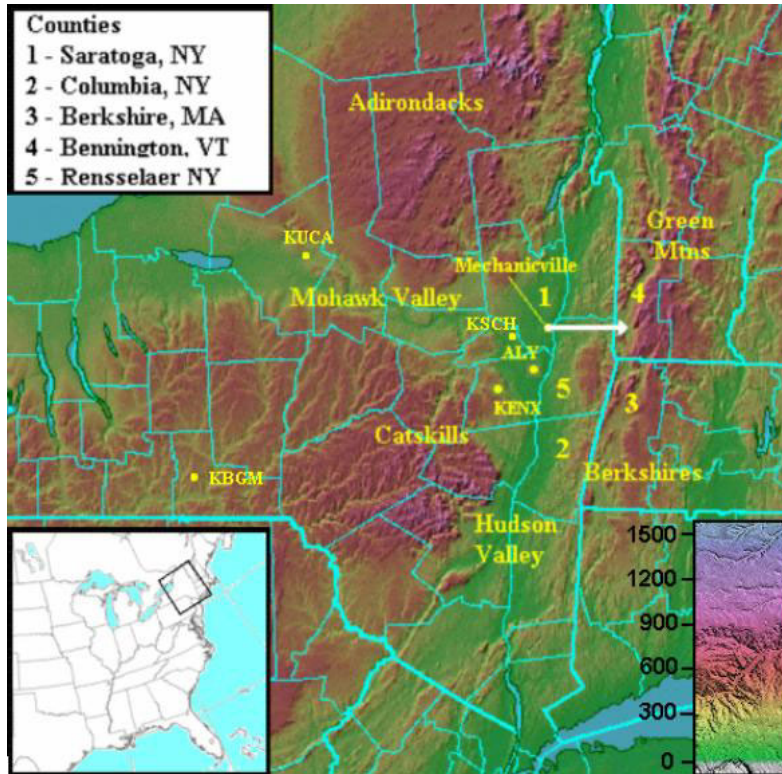


Fig. 1. Map of eastern NY and western New England showing terrain features. The white arrow indicates the path of the Mechanicville tornado, KENX is the NWS radar location, and ALY is the location of the Albany NWS radiosonde site. Terrain heights (m) according to color bar in the lower right. The terrain map was obtained online from the Color Landform Atlas of North America, compiled by Ray Sterner of Johns Hopkins University Applied Physics Laboratory (<http://fermi.jhuapl.edu/states/states.html>)

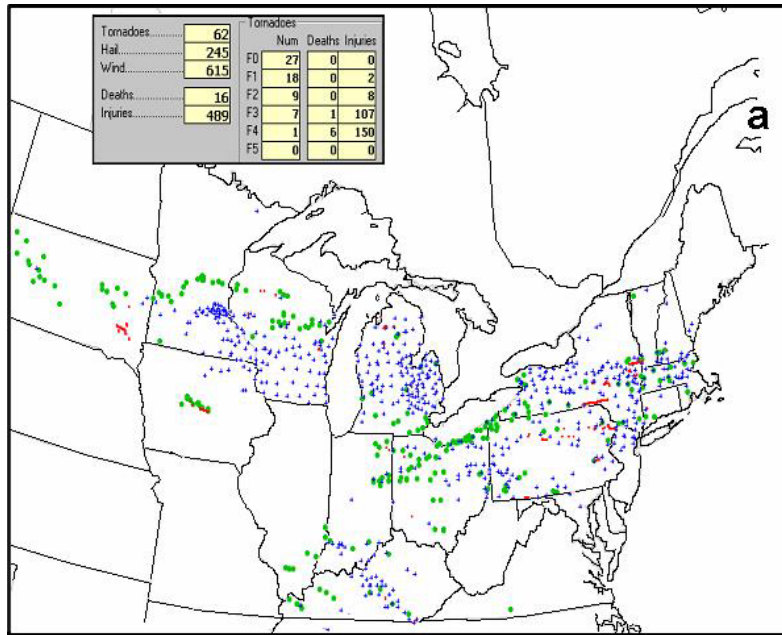


Fig. 2. Severe weather reported across the northern United States from 1800 UTC 30 May to 0400 UTC 1 June 1998 (Hart and Janish 1999). Tornadoes are indicated by red dots or lines, hail by green dots and severe wind reports by blue crosses.

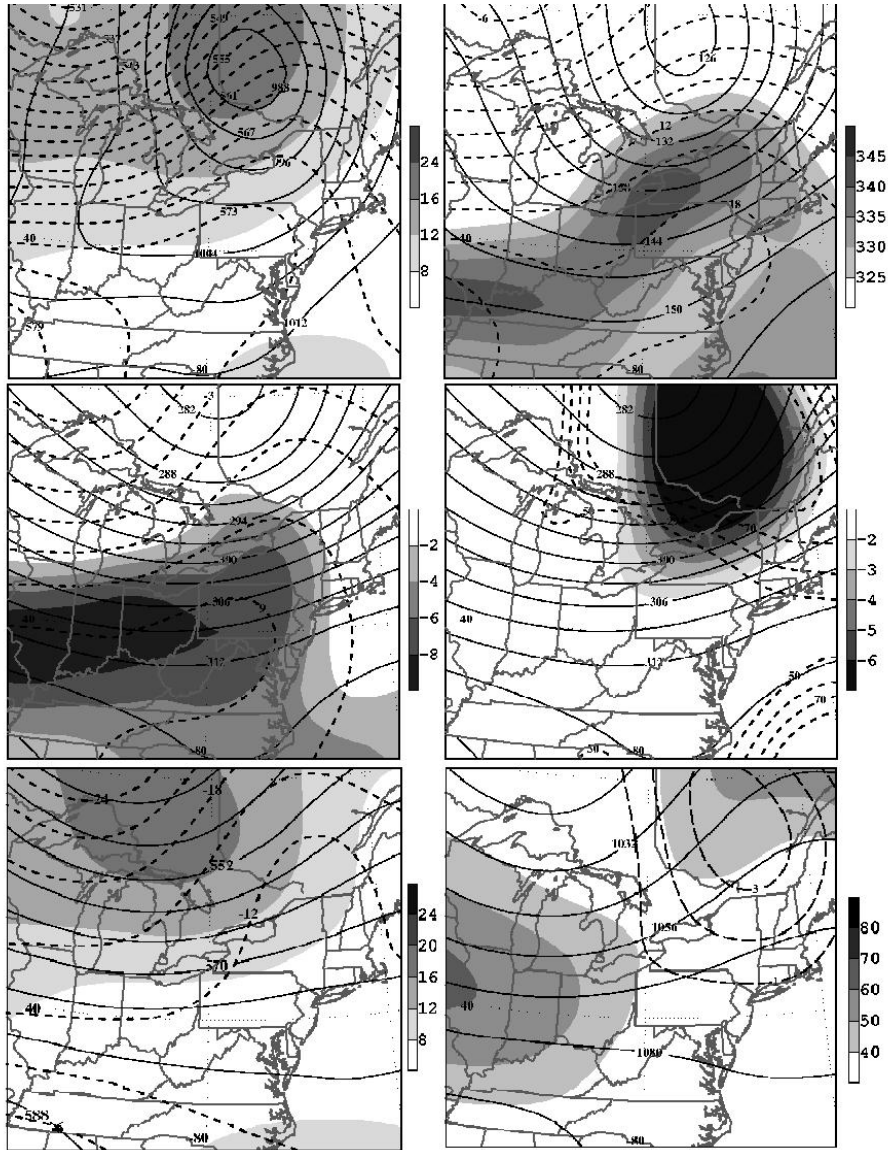


Fig. 3. 1800 UTC 31 May analyses for (a) Sea-level pressure (solid, every 4 hPa), 1000-500 hPa thickness (dashed, every 3 dam) and 700 hPa absolute vorticity (every $4 \times 10^{-5} \text{ s}^{-1}$ beginning at $8 \times 10^{-5} \text{ s}^{-1}$ and shaded according to the gray scale) for 1800 UTC 31 May. (b) 850 hPa geopotential heights (solid, every 3 dam), temperatures (dashed, every 3°C) and θ_e (every 5 K beginning at 325 K and shaded according to the gray scale). (c) 700 hPa geopotential heights (solid, every 3 dam), temperature (dashed, every 3°C) and lifted index (LI) (shaded according to the gray scale for values < -2). (d) 700 hPa geopotential heights (solid, every 3 dam), 700 hPa relative humidity (dashed, every 10% beginning at 50%) and 700 hPa ascent (every $2 \times 10^{-3} \text{ hPa s}^{-1}$ beginning at $-2 \times 10^{-3} \text{ hPa s}^{-1}$ and shaded according to the gray scale). (e) 500 hPa geopotential heights (solid, every 3 dam), temperature (dashed, every 3°C) and absolute vorticity (every $4 \times 10^{-5} \text{ s}^{-1}$ beginning at $8 \times 10^{-5} \text{ s}^{-1}$ and shaded according to the gray scale). (f) 250 hPa geopotential heights (solid, every 12 dam), divergence (dashed, positive values only, every $1 \times 10^{-5} \text{ s}^{-1}$) and isotachs (every 10 m s^{-1} beginning at 40 m s^{-1} and shaded according to the gray scale).

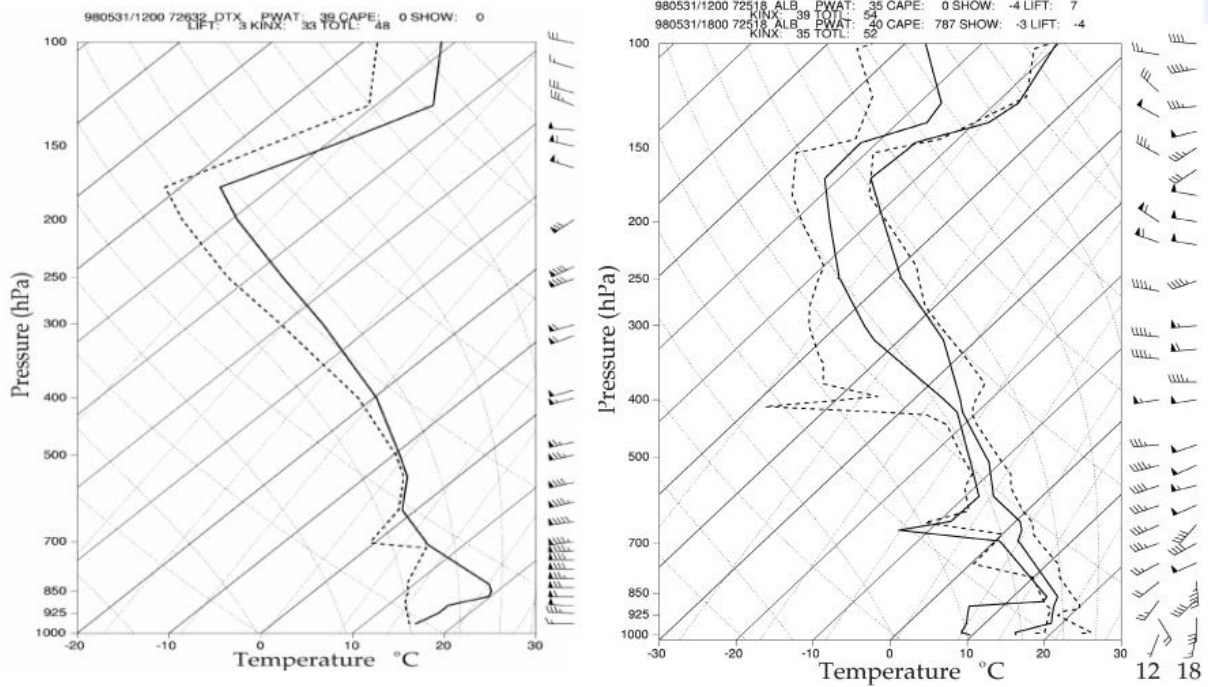


Fig. 4. (a) Sounding (skew T-log p format) for DTX (72632) for 1200 UTC 31 May 1998. Winds in m s^{-1} with one pennant, full barb and half barb denoting 25 m s^{-1} , 5 m s^{-1} , and 2.5 m s^{-1} , respectively. (b) As in (a) except for ALY (72518) for 1200 (solid) and 1800 (dashed) UTC 31 May 1998.

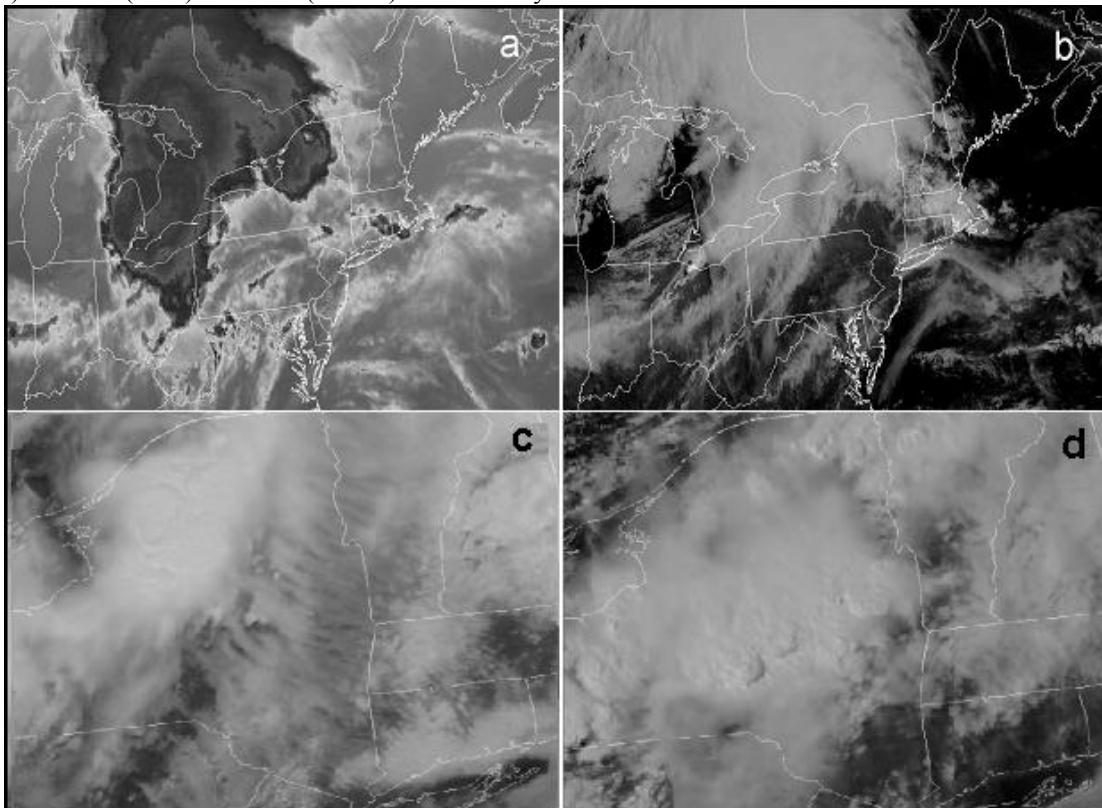


Fig. 5. Satellite imagery on 31 May 1998 with (a) infrared image at 1215 UTC, and visible images at (b) 1402 UTC, (c) 1702 UTC and (d) 2002 UTC.

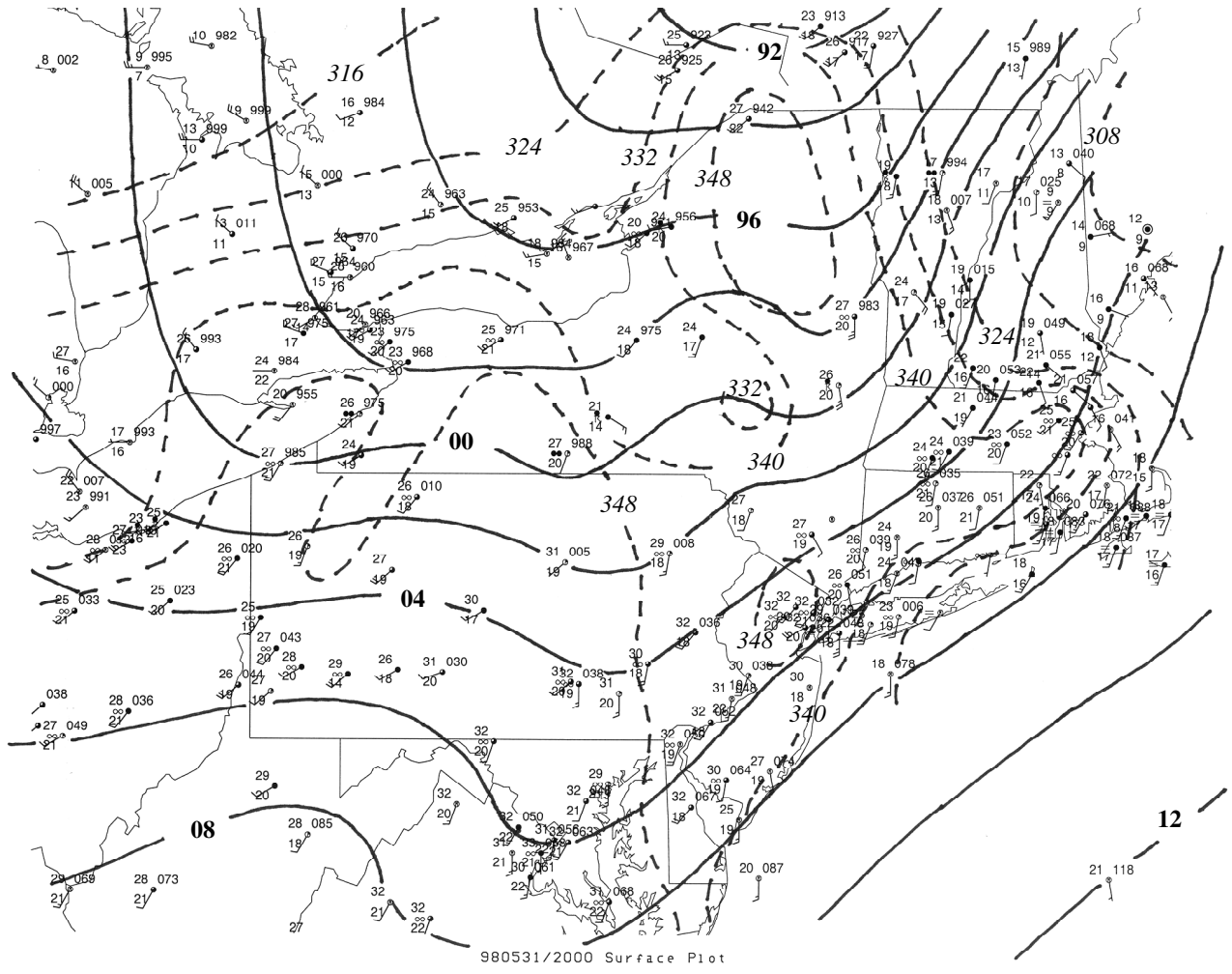


Fig. 6. Manual analysis of sea-level pressure (solid contours every 2 hPa) and θ_e (dashed contours every 8 K) for 1500 UTC 31 May 1998.

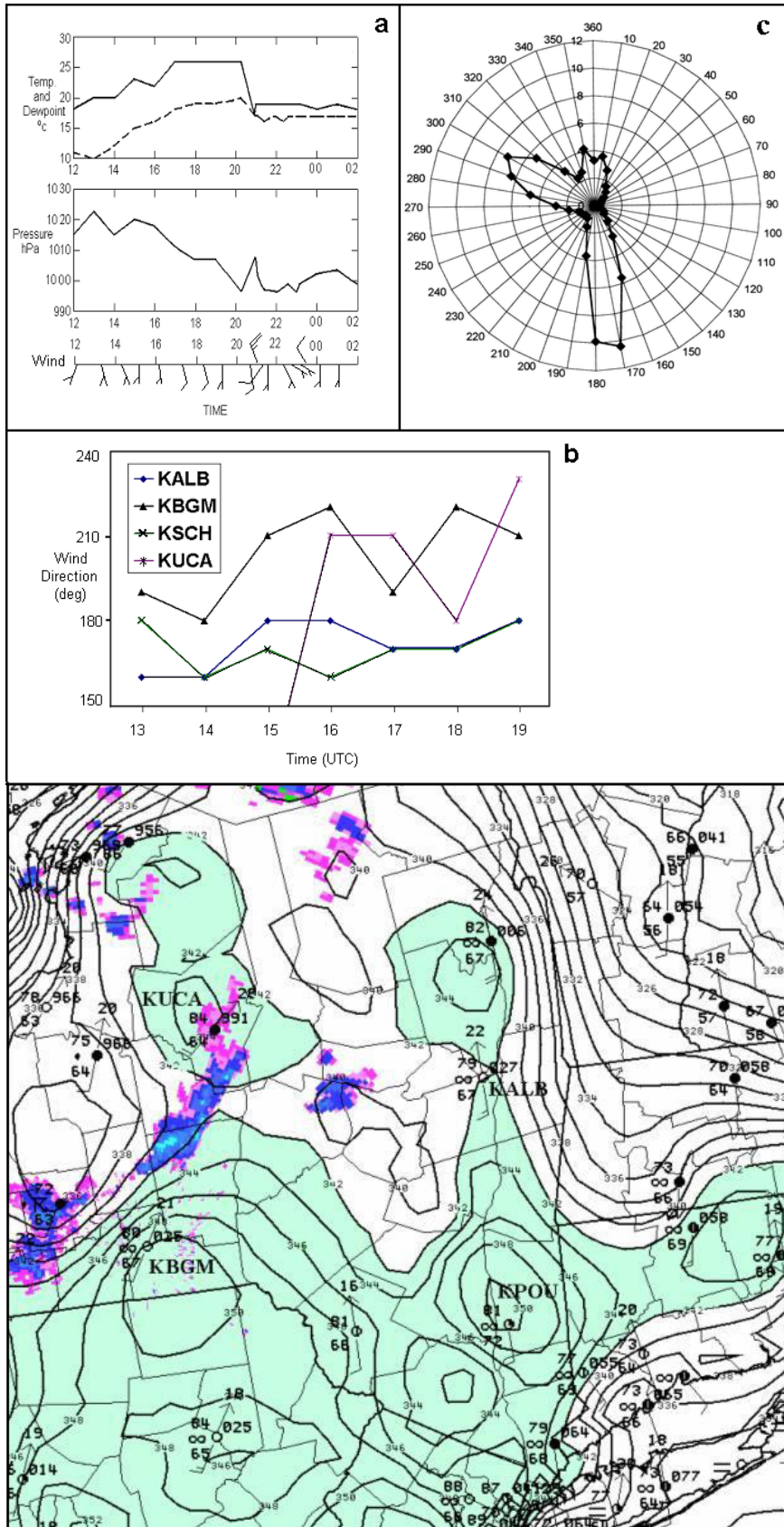
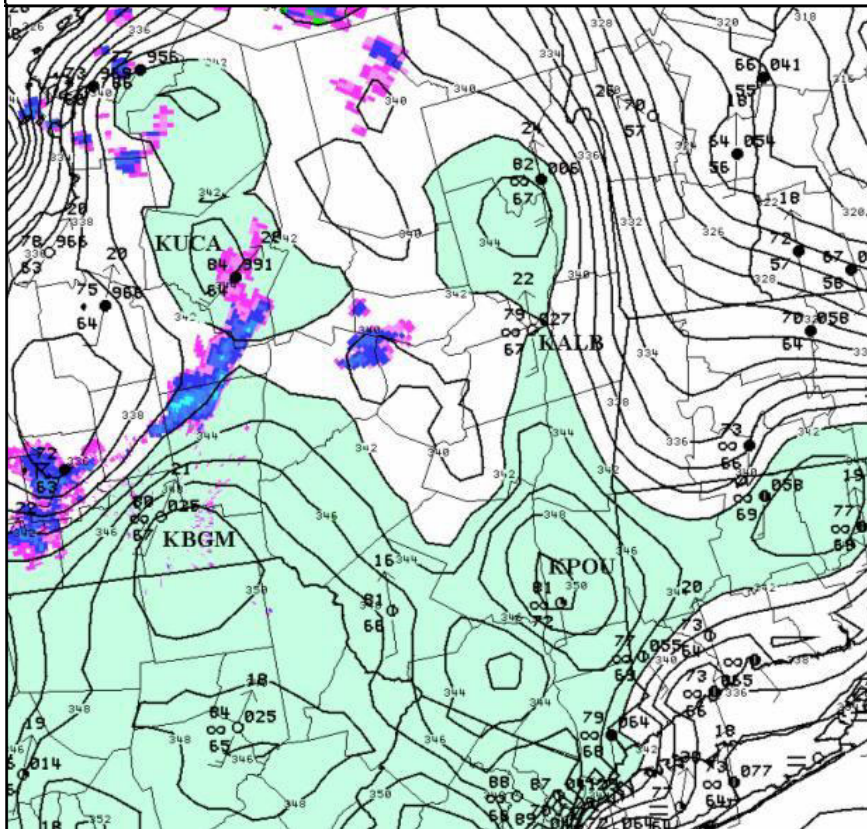


Fig. 7. (a) Time series (UTC) of temperatures (solid) and dewpoint (dashed) in °C (top graph), (b) pressure in hPa (middle graph), and wind (as in Figs. 8a,b) for KALB on 31 May 1998. KALB is located about 6 km north of the ALY radiosonde site. (b) Time series comparing wind direction at KALB and KSCH in the Hudson Valley with KUCA and KBGM located west of the Hudson Valley (see Fig. 1). (c) Wind rose for KALB for the period March 1993 to March 1997 taken from Wasula et al. (2002).

Fig. 8. AWIPS LAPS analysis of surface θ_e at 1900 UTC 31 May 1998. Light green shaded areas represent θ_e values > 342 K. Radar reflectivity (0.5° elevation scan, greater than 20 dBZ) according to color bar at the top. Conventional plotting of surface observations except temperature and dew point values are given in °F.



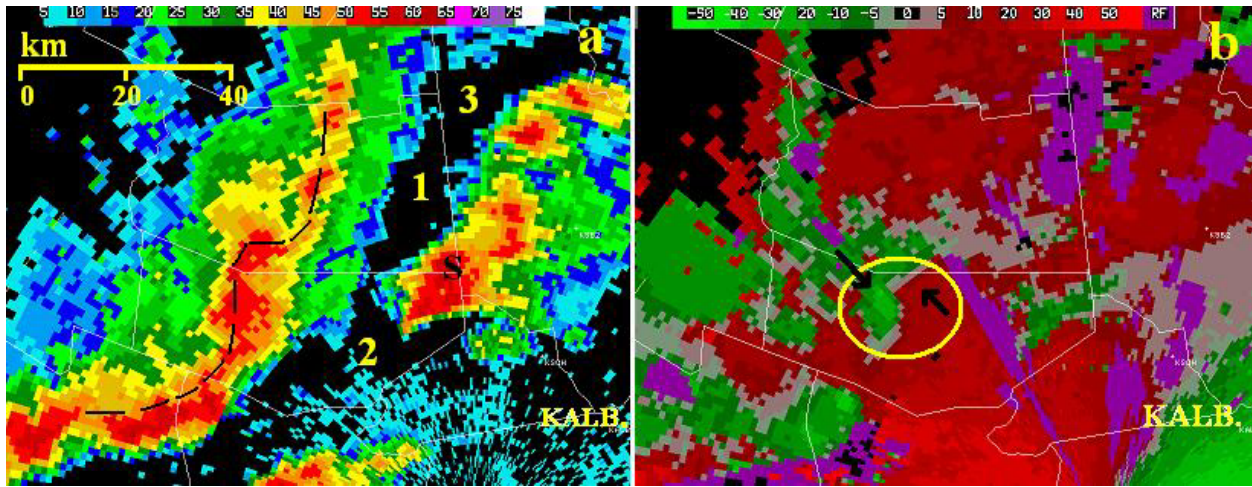


Fig. 9. (a) KENX reflectivity (dBZ) at 1946 UTC 31 May 1998 according to the color bar at the top. The letter S indicates the location of the supercell that produced the Mechanicville tornado. The dashed line marks the line of thunderstorms to the west with the associated LEWP. The numbers 1, 2 and 3 indicate the locations of Fulton, Montgomery and Saratoga Counties, respectively. (b) KENX SRM (kt) at 1946 UTC according to the color bar at the top with the yellow circle indicating the location of mesoscale vortex. The KENX radar is located near the lower right portion of the figure.

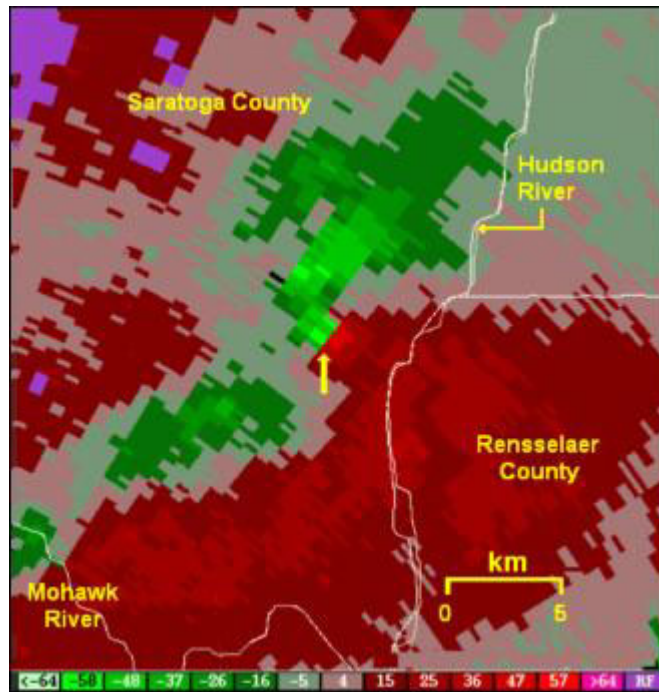


Fig.10. (a) KENX 0.5° SRM at 2022 UTC 31 May (tornado formation time).

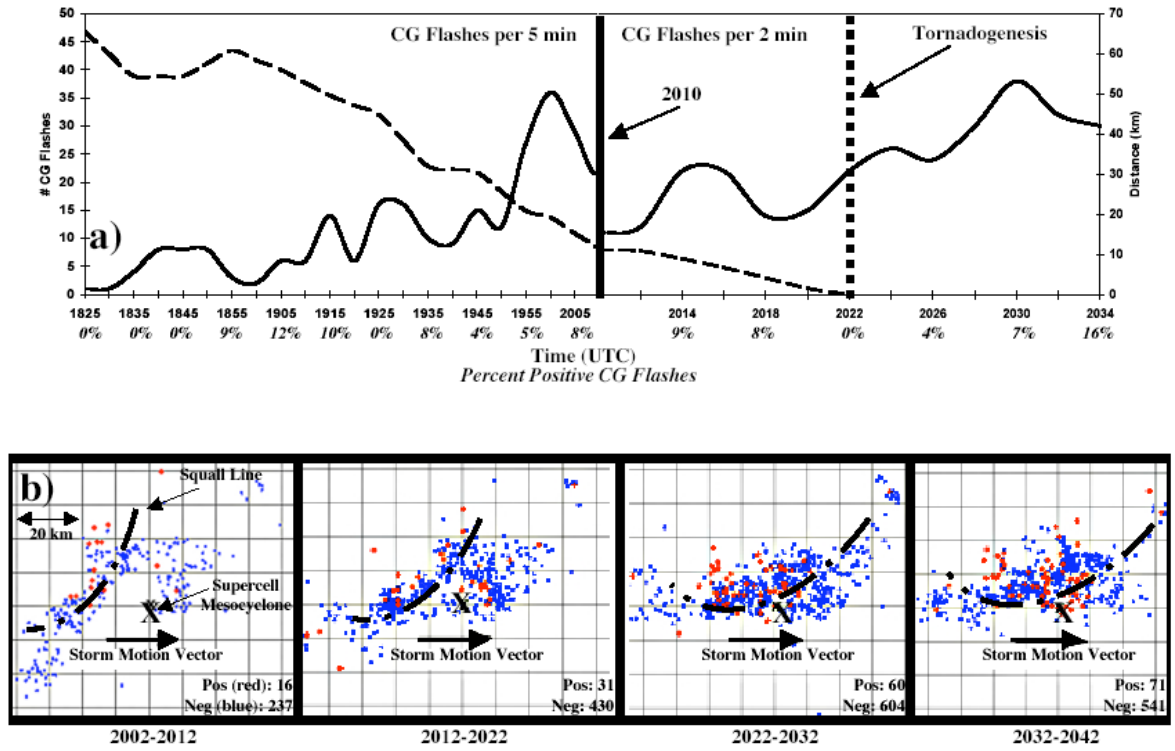


Fig. 11. (a) CG lightning strikes at 2 minute intervals with times in minutes and t representing tornado formation time. (b) CG lightning from 2002 to 2042 UTC on 31 May 1998 plotted relative to the mesocyclone center which is marked by the X at the center of the figure. The storm motion ($260^\circ 21 \text{ m s}^{-1}$) is along the horizontal axis. Dots indicate negative CG lightning strikes and pluses positive strikes. Purple indicates lightning from 2002-2012 UTC, blue from 2012-2022 UTC, green from 2022-2032 UTC and red from 2032-2042 UTC.